arXiv:2512.15146v4 [cs.CL] 6 May 2026

Beyond Majority Voting: Towards Fine-grained and More Reliable Reward Signal for Test-Time Reinforcement Learning

Weiqin Wang[1], **Yile Wang**[1,✉], **Kehao Chen**[2], **Hui Huang**[1]
[1]College of Computer Science and Software Engineering, Shenzhen University
[2]College of Computer and Data Science, Fuzhou University
here1swqw@gmail.com, wangyile@szu.edu.cn

Abstract

Test-time reinforcement learning mitigates the reliance on annotated data by using *majority voting* results as pseudo-labels, emerging as a complementary direction to reinforcement learning with verifiable rewards (RLVR) for improving reasoning ability of large language models (LLMs). However, this voting strategy often induces *confirmation bias* and suffers from *sparse rewards*, limiting the overall performance. In this work, we propose subgroup-specific step-wise confidence-weighted pseudo-label estimation (SCOPE), a framework integrating model confidence and dynamic subgroup partitioning to address these issues. Specifically, SCOPE integrates the proposed step-wise confidence into pseudo-label estimation, prioritizing high-quality reasoning paths over simple frequency count. Furthermore, it dynamically partitions the candidate outputs pool into independent subgroups by balancing reasoning quality against exploration diversity. By deriving local consensus via repeat sampling for each subgroup, SCOPE provides diverse supervision targets to encourage broader exploration. We conduct experiments across various models and benchmarks, experimental results show that SCOPE consistently outperforms recent baselines. Notably, SCOPE achieves relative improvements of 13.1% on challenging AIME 2025 and 8.1% on AMC. The code is released at https://github.com/szu-tera/SCOPE.

1 Introduction

Reinforcement learning (RL) has become an important paradigm in improving the reasoning capability of large language models (LLMs). The paradigm of reinforcement learning with verifiable rewards (RLVR) has also been used in seminal models such as DeepSeek-R1 (DeepSeek-AI, 2025), Qwen3 (Yang et al., 2025), and OpenAI's o1 (OpenAI, 2024). From the perspective of training data, RLVR is similar to supervised fine-tuning that requires ground-truth labels to guide the iterative policy learning process and thus elicit the strong reasoning ability of LLMs (Wen et al., 2025; Su et al., 2025; Tang et al., 2025).

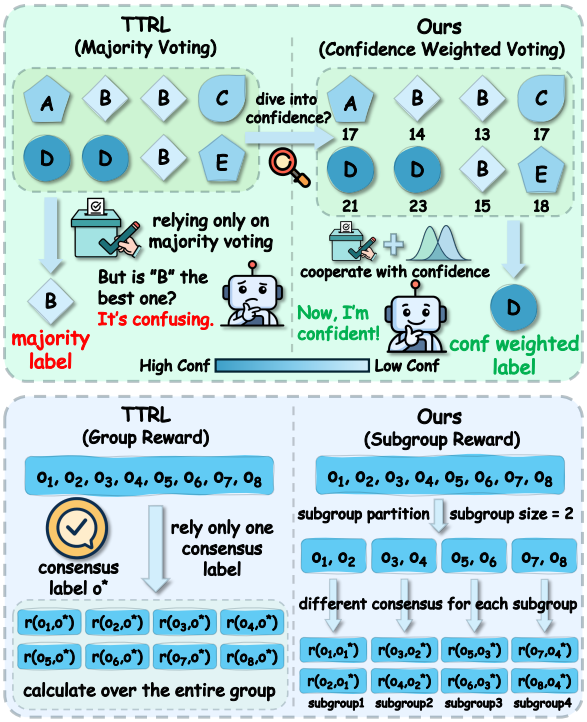

Figure 1: Illustration of the difference betweens TTRL (Zuo et al., 2025) and our method. Top: consensus label estimation with step-wise confidence weighting. Bottom: group partition and reward calculation using subgroup-specific consensus labels.

However, dependence on extensive manual labeling is costly and inefficient, especially for large-scale or complex tasks. Thus, there are studies that try to enable reinforcement learning of LLMs without supervision. Zuo et al. (2025) proposed test-time reinforcement learning (TTRL) that samples multiple responses from the policy model and then employs majority voting to obtain a consensus label to replace a predefined ground-truth label,

✉Corresponding author.

enabling LLMs to be trained directly in real-world settings without supervision.

While TTRL provides a straightforward and effective framework for unsupervised RL, its reliance on majority voting for pseudo-label generation represents a significant bottleneck. This coarse-grained estimation process treats all votes equally regardless of their underlying confidence, leading to two critical issues: (1) *confirmation bias*, where the model risks reinforcing its own errors from incorrect label estimation (Arazo et al., 2020; Prabhu et al., 2021; Wang et al., 2025c), particularly when the majority consensus aligns with a plausible but incorrect answer; and (2) *sparse rewards*, as the binary nature of voting fails to capture dense, fine-grained signals essential for fine-tuning (Lightman et al., 2024). While recent advances have successfully leveraged step-wise mechanisms to optimize test-time reasoning efficiency (Huang et al., 2026), utilizing such fine-grained signals to improve test-time reward reliability remains largely underexplored.

To mitigate the above limitations of TTRL, we propose subgroup-specific step-wise confidence-weighted pseudo-label estimation (SCOPE). First, SCOPE introduces step-wise confidence for pseudo-label estimation to address the issue of potentially incorrect label estimation. Figure 1 (Top) shows an example of eight responses where the vote counts for solution A∼E are 1, 3, 1, 2, and 1, respectively. The majority voting strategy selects solution B, as it receives the highest number of votes. However, a step-wise confidence analysis reveals that solution B exhibit low confidence (i.e., high uncertainty). In contrast, solution D demonstrates higher accumulated confidence and is the correct solution, though having less vote counts. Second, we design a subgroup-specific pseudo-label estimation strategy to alleviate the issue of sparse rewards. Unlike TTRL, which assigns a uniform pseudo-label to all sampled responses for reward calculation, our method partitions the responses into distinct subgroups, assigning a separate label to each subgroup, as shown in Figure 1 (Bottom). Moreover, we employ Pareto optimization (Pareto, 1964) to automatically select the optimal subgroup size during training.

We validate our method on advanced LLMs, including LLaMA3.1 (Grattafiori et al., 2024), Qwen2.5 (Yang et al., 2024), and Qwen3 (Yang et al., 2025) with different parameter sizes. Empirical results demonstrate that SCOPE consistently outperforms baselines. In particular, applying SCOPE to Qwen3-8B yields an improvement on AIME 2024 (Li et al., 2024) of 10.48%, with an average gain of 6.85% across all benchmarks.

Our contributions are summarized as follows:

- We propose SCOPE, a novel test-time reinforcement learning framework that leverages step-wise confidence weighting and subgroup-specific label estimation to mitigate the limitations of sparse rewards and confirmation bias in unsupervised RL.
- We introduce step-wise confidence to recover correct answers in the minority and Pareto-optimized subgroups to balance reward density and estimation accuracy during training.
- Extensive experiments demonstrate the effectiveness of SCOPE in improving reasoning capabilities, achieving superior performance across multiple benchmarks.

2 Preliminaries

2.1 Group Relative Policy Optimization

Group Relative Policy Optimization (GRPO; Shao et al., 2024) estimates the advantage of a policy by leveraging group-wise relative rewards, eliminating the need for a separate value function. Given a group of candidate outputs $\{o_i\}_{i=1}^{|\mathcal{G}|}$ sampled from the old policy $\pi_{\theta_{\text{old}}}$ for an input $\mathbf{x}$, GRPO computes the advantage $\mathcal{A}_i$ for each response o_i:

$$\mathcal{A}_i = \frac{r(o_i) - \mu_g}{\sigma_g + \epsilon}, \tag{1}$$

and $r(o_i)$ denotes the reward for response o_i. μ_g, σ_g represent the mean and standard deviation of the rewards within the group, respectively. ϵ is a small constant added for numerical stability. Subsequently, the policy model π_θ is optimized by maximizing the following surrogate objective:

$$\begin{aligned}\mathcal{J}_{\text{GRPO}}(\theta) = \mathbb{E}_{\mathbf{x},\{o_i\}\sim\pi_{\text{old}}}\Bigg[\frac{1}{|\mathcal{G}|}\sum_{i=1}^{|\mathcal{G}|}\frac{1}{|o_i|}\sum_{t=1}^{|o_i|}\Big(\\ \min\Big[\rho_{i,t}\mathcal{A}_i, \text{clip}(\rho_{i,t}, 1-\epsilon, 1+\epsilon)\mathcal{A}_i\Big]\\ -\beta\mathbb{D}_{\text{KL}}[\pi_\theta||\pi_{\text{ref}}]_t\Big)\Bigg],\end{aligned} \tag{2}$$

where $\rho_{i,t} = \frac{\pi_\theta(o_{i,t}|\mathbf{x}, o_{i,<t})}{\pi_{\theta_{\text{old}}}(o_{i,t}|\mathbf{x}, o_{i,<t})}$ represents the probability ratio between the current and old policies at step t, β is the coefficient for the KL divergence penalty, and π_{ref} is the reference model used to prevent excessive policy deviation.

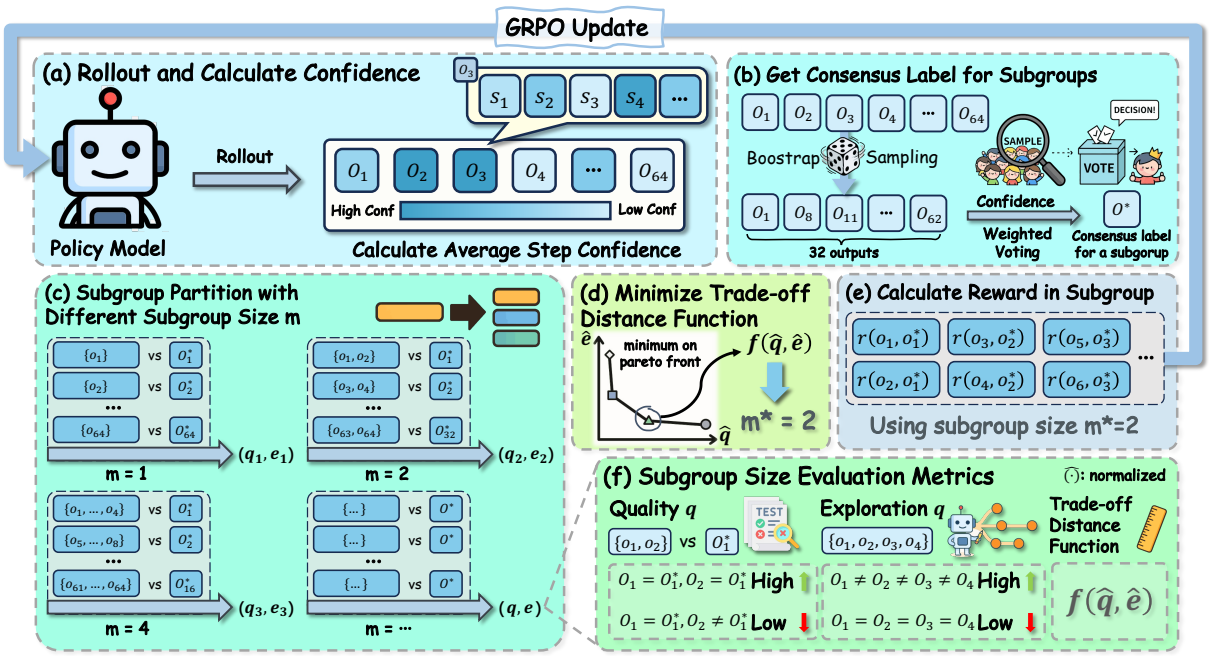

Figure 2: Overview of the SCOPE framework. The process involves **(a)** generating responses with step-wise confidence, **(b)** estimating consensus labels via weighted voting, **(c)** evaluating different subgroup partitions, **(d)** employing Pareto optimization to select the optimal subgroup size m^* by balancing **(f)** quality and exploration metrics, and **(e)** computing rewards using the optimized subgroup strategy for model updates.

2.2 Test-Time Reinforcement Learning

Zuo et al. (2025) proposed TTRL to mitigate the dependence on ground-truth labels g, which are traditionally required in the reward function $r(o_i, g)$. The core idea is to replace external supervision by leveraging the majority voting result over a group of sampled outputs $\{o_i\}_{i=1}^{|\mathcal{G}|}$ to derive a consensus label o^*:

$$o^* = \underset{o}{\operatorname{argmax}} \sum_{i=1}^{|\mathcal{G}|} \mathbb{1}(o_i = o), \tag{3}$$

where consensus output o^* serves as a *pseudo-label*, allowing the reward to be computed through $r(o_i, o^*)$ without requiring ground-truth labels.

2.3 Token Confidence

Recent studies indicate that LLMs exhibit varying levels of confidence during the reasoning process, and token confidence is often utilized as a metric to quantify the local certainty of a language model's prediction at a specific step (Fu et al., 2025). Given the predicted probability distribution at position i, the token confidence $\mathcal{C}_i$ is defined as the negative average log-probability of the top-k most probable tokens:

$$\mathcal{C}_i = -\frac{1}{k} \sum_{j=1}^{k} \log P_i(j), \tag{4}$$

where $P_i(j)$ denotes the probability of the j-th candidate among the top-k tokens during decoding. Conceptually, a higher $\mathcal{C}_i$ implies that the probability mass is concentrated on a few tokens with a peaked distribution, indicating high certainty. Conversely, a lower value reflects a flatter distribution, suggesting that the model is uncertain about the next token prediction.

3 Method

Figure 2 shows the overall pipeline of SCOPE. We begin by introducing the *average step confidence* (§3.1) and its calculation method. Next, we propose the concept of *subgroup* (§3.2) and its detailed formulation. Subsequently, we describe how to adaptively determine the optimal subgroup size during training via *Pareto optimization* (§3.3). Finally, we provide the *unified algorithm* of SCOPE that integrates the above key components (§3.4).

3.1 Thinking with Step Confidence

We first propose **Average Step Confidence** to capture fine-grained uncertainty of LLMs during reasoning. This metric is designed to balance the reward signals with different granularity, avoiding the excessive noise often observed in raw token-level probabilities while retaining structural precision. Specifically, we decompose a response o_i into

a sequence of reasoning steps by newline delimiter "\n\n", denote as $o_i = s_1, ..., s_k, ..., s_{|\mathcal{L}|}$, with length $|\mathcal{L}|$. The confidence for each step s_k is then calculated by averaging the confidence scores of its constituent tokens:

$$\mathcal{C}_{s_k} = \frac{1}{N_k} \sum_{t=1}^{N_k} \mathcal{C}_t, \tag{5}$$

where N_k denotes the number of tokens in the k-th step s_k, and $\mathcal{C}_t$ represents the confidence score of the t-th token within that step, as calculated in Eq. 4. To quantify the overall certainty of the response o_i, we compute the average step confidence by aggregating the step-level scores:

$$\mathcal{C}^{(i)}_{\text{AvgStep}} = \frac{1}{|\mathcal{L}|} \sum_{k=1}^{|\mathcal{L}|} \mathcal{C}_{s_k}, \tag{6}$$

where $|\mathcal{L}|$ is the total number of steps in o_i. Finally, as shown in Figure 2(b), we employ these confidence scores as weights to estimate the consensus label. Unlike naive majority voting, our method assigns higher importance to responses with higher average step confidence:

$$o^* = \underset{y}{\operatorname{argmax}} \sum_{i=1}^{|\mathcal{G}|} \mathcal{C}^{(i)}_{\text{AvgStep}} \cdot \mathbb{1}\left[\text{Ans}(o_i) = y\right], \tag{7}$$

where $\text{Ans}(o_i)$ denotes the final answer extracted from response o_i, and the maximization is performed over all unique candidate answers y. Here, o^* represents the consensus label derived via confidence-weighted voting. By prioritizing candidates based on reasoning certainty rather than simple frequency, o^* serves as a robust, confidence-aware target for reward calculation, superseding majority voting. Besides step-level confidence, we compare different confidence granularities in §5.2.

3.2 Fine-grained Rewards within Subgroups

Instead of relying on a single consensus derived from the entire set of outputs $\{o_i\}_{i=1}^{|\mathcal{G}|}$, which can be sparse, we define a granular unit for reward computation, referred to as a **Subgroup**. As illustrated in Figure 2(c), we partition the global pool of $|\mathcal{G}|$ generated responses into distinct subgroups, each containing $m = |\mathcal{G}|/n$ outputs. The set of subgroups can be formally denoted as:

$$\mathcal{S} = \left\{ S_j = \{o_{(j-1)m+1}, \ldots, o_{jm}\} \right\}_{j=1}^{n}. \tag{8}$$

To derive the consensus label o_j^* for each subgroup S_j, we employ an independent estimation strategy. Specifically, as depicted in Figure 2(b), for each of the n subgroups, we perform bootstrap sampling from the global pool of generated responses $\{o_i\}_{i=1}^{|\mathcal{G}|}$ to construct a candidate set. We then apply the confidence-weighted voting mechanism described in §3.1 to this set to determine o_j^*. Consequently, the label estimation process is executed n times, each corresponding to a distinct subgroup. This strategy enables subgroups to explore diverse reasoning paths while ensuring each receives a robust consensus target derived from the global distribution.

Finally, as shown in Figure 2(e), the correctness reward for each output $o \in S_j$ is computed against its corresponding subgroup-specific consensus o_j^*:

$$r(o, o_j^*) = \mathbb{1}\left[\text{Ans}(o) = o_j^*\right]. \tag{9}$$

3.3 Automatic Subgroup Size Selection with Pareto Optimization

Having defined the subgroup mechanism, we now detail the procedure for automatically selecting the optimal subgroup size m during training. As illustrated in Figure 2(f), this selection process aims to balance two competing objectives: (1) **Reasoning Quality**: ensuring output correctness by maximizing alignment with the local consensus; and (2) **Exploration**: preserving solution diversity to avoid overconfidence and mode collapse.

To quantify these objectives, we formulate two metrics. The first is the *quality rate* q, which measures the consistency of outputs with their subgroup consensus:

$$q = \frac{1}{|\mathcal{G}|} \sum_{j=1}^{n} \sum_{l=1}^{m} \mathbb{1}\left[\text{Ans}(o_{(j-1)m+l}) = o_j^*\right], \tag{10}$$

where $|\mathcal{G}|$ is the total number of generated outputs, n is the number of subgroups, and o_j^* denotes the consensus label of the j-th subgroup. The second metric is the *exploration rate* e, defined as the proportion of unique consensus labels discovered:

$$e = \frac{\left|\{\, o_1^*, o_2^*, \ldots, o_n^* \,\}\right|}{n}, \tag{11}$$

where o_j^* is the consensus label of the j-th subgroup, and $|\cdot|$ denotes the cardinality of the set of unique consensus outputs across all subgroups.

As depicted in Figure 2(c), we evaluate a set of candidate subgroup sizes (e.g., $m = 1, 2, 4, \ldots$) by

computing their corresponding pairs (q_k, e_k). Inspired by previous work (Zhong et al., 2024; Lou et al., 2025), we formulate this selection process as an optimization problem. In particular, we construct a Pareto front $\{(q_k, e_k)\}_{k=1}^{P}$ from these candidates to identify non-dominated solutions. To select the final optimal size m^*, we compute a *trade-off distance* for each Pareto-optimal point, as shown in Figure 2(d). We first normalize the metrics:

$$\hat{q}_k = \frac{q_k - q_{\min}}{q_{\max} - q_{\min}}, \quad (12)$$

$$\hat{e}_k = \frac{e_k - e_{\min}}{e_{\max} - e_{\min}}. \quad (13)$$

Then, we compute the weighted trade-off distance d_k for each candidate point to the ideal state:

$$d_k = \sqrt{\lambda(1 - \hat{q}_k)^2 + (1 - \lambda)(1 - \hat{e}_k)^2}, \quad (14)$$

where $\lambda \in [0, 1]$ is a trade-off parameter that controls the preference between quality and exploration. We set $\lambda = 0.7$ in our experiments, and a detailed analysis of this parameter selection is provided in §5.1. Finally, we select the optimal subgroup size m^* that minimizes this distance:

$$m^* = \operatorname*{argmin}_{m_k} d_k. \quad (15)$$

3.4 The Unified Algorithm

We summarize the complete training procedure of SCOPE in Algorithm 1. In each iteration, the policy model first generates a pool of candidate responses for a given input, and we compute the average step confidence for each response (§3.1). To dynamically balance the trade-off between reasoning quality and exploration, SCOPE evaluates multiple subgroup configurations and selects the optimal subgroup size m^* via Pareto optimization (§3.3). Subsequently, the responses are partitioned into subgroups based on m^*, where local consensus labels are derived using step-wise confidence-weighted voting with bootstrap sampling (§3.2). Finally, fine-grained rewards are computed against local targets to update the policy via GRPO.

Algorithm 1 Training Iteration of SCOPE

Require: Input dataset $\mathcal{D}$, Policy π_θ, Candidate sizes $\mathcal{M}$.
Sample $\mathbf{x} \sim \mathcal{D}$ and rollout $\{o_i\}_{i=1}^{|\mathcal{G}|} \sim \pi_\theta(\cdot|\mathbf{x})$.
Calculate average step confidence $\mathcal{C}_{\text{AvgStep}}^{(i)}$ for each output.
// Automatic Subgroup Size Selection
Evaluate quality q and exploration e for all $m \in \mathcal{M}$.
Select optimal subgroup size m^* by minimizing the trade-off distance on the Pareto front.
// Subgroup-specific Reward Computation
Partition $\{o_i\}_{i=1}^{|\mathcal{G}|}$ into subgroups $\{S_j\}$ of size m^*.
for each subgroup S_j **do**
  Derive local consensus o_j^* via bootstrap sampling and confidence-weighted voting.
  Set rewards $r_i \leftarrow \mathbb{1}[\text{Ans}(o_i) = \text{Ans}(o_j^*)]$ for $o_i \in S_j$.
end for
Update π_θ using GRPO objective with computed rewards.

4 Experiments

4.1 Experimental Settings

Models. We evaluate the generalization ability of SCOPE through comprehensive experiments on a diverse set of widely used LLMs, covering a broad spectrum from lightweight to medium-scale parameter sizes. The models included in our experiments are as follows: QWEN2.5-MATH-1.5B (Yang et al., 2024), QWEN3-1.7B, QWEN3-8B (Yang et al., 2025), and LLAMA3.1-8B-INSTRUCT (Grattafiori et al., 2024). The checkpoints are listed in Appendix A.

Evaluation. We evaluate SCOPE on four representative benchmarks: **AIME 2024** (Li et al., 2024), **AIME 2025** (Li et al., 2024), **AMC** (Li et al., 2024), and **MATH-500** (Hendrycks et al., 2021). We list dataset examples in Appendix B and evaluation details in Appendix C.

Baselines. We adopt **TTRL** (Zuo et al., 2025) with majority voting to get a consensus label as our primary baseline. Besides, we also compare following methods: (1) **INTUITOR** (Zhao et al., 2025) uses self-certainty (internal confidence) as intrinsic rewards for unsupervised RL training; (2) **RLPR** (Yu et al., 2025) uses the model's intrinsic probability of generating the reference answer as a reward signal to extend RLVR to general domains without external verifiers; (3) **CO-REWARDING-I** (Zhang et al., 2025) generates reward signals by enforcing contrastive agreement between the model's reasoning outputs on original questions and their semantically equivalent rephrased counterparts; and (4) **EVOL-RL** (Zhou et al., 2025) combines majority voting for stability with a semantic novelty reward to encourage diverse reasoning paths. The training details are shown in Appendix C.

4.2 Main Results

The results are shown in Table 1. Overall, our method consistently achieves superior performance

Models	AIME 2024	AIME 2025	AMC	MATH-500	Avg
I. LIGHTWEIGHT-SIZED MODELS					
QWEN2.5-MATH-1.5B					
QWEN2.5-MATH-1.5B (Yang et al., 2024)	$7.92_{\pm 0.11}$	$3.12_{\pm 0.08}$	$26.58_{\pm 0.29}$	$32.21_{\pm 0.33}$	17.46
w/ INTUITOR (Zhao et al., 2025)	$6.88_{\pm 0.12}$	$5.50_{\pm 0.07}$	$39.08_{\pm 0.25}$	$64.26_{\pm 0.21}$	28.93
w/ TTRL (Zuo et al., 2025)	$\underline{16.48}_{\pm 0.12}$	$\underline{9.86}_{\pm 0.12}$	$\underline{48.87}_{\pm 0.17}$	$\underline{72.58}_{\pm 0.16}$	$\underline{36.95}$
w/ SCOPE (Ours)	$\mathbf{22.50}_{\pm 0.11}$	$\mathbf{14.90}_{\pm 0.03}$	$\mathbf{51.20}_{\pm 0.15}$	$\mathbf{76.85}_{\pm 0.09}$	**41.36**
Δ	↑ 6.02/36.5%	↑ 5.04/51.1%	↑ 2.33/4.8%	↑ 4.27/5.9%	↑ 4.40/11.9%
QWEN3-1.7B					
QWEN3-1.7B (Yang et al., 2025)	$11.45_{\pm 0.11}$	$11.53_{\pm 0.11}$	$39.30_{\pm 0.26}$	$73.23_{\pm 0.17}$	33.88
w/ INTUITOR (Zhao et al., 2025)	$15.18_{\pm 0.04}$	$11.42_{\pm 0.08}$	$45.58_{\pm 0.19}$	$76.11_{\pm 0.13}$	37.07
w/ CO-REWARDING-I (Zhang et al., 2025)	$16.42_{\pm 0.08}$	$12.19_{\pm 0.10}$	$\underline{51.99}_{\pm 0.13}$	$\underline{78.91}_{\pm 0.09}$	39.88
w/ TTRL (Zuo et al., 2025)	$\underline{19.37}_{\pm 0.09}$	$\underline{19.23}_{\pm 0.01}$	$50.45_{\pm 0.08}$	$78.18_{\pm 0.07}$	$\underline{41.91}$
w/ SCOPE (Ours)	$\mathbf{21.66}_{\pm 0.05}$	$\mathbf{19.71}_{\pm 0.02}$	$\mathbf{53.46}_{\pm 0.05}$	$\mathbf{81.27}_{\pm 0.05}$	**44.02**
Δ	↑ 2.29/11.8%	↑ 0.48/2.5%	↑ 3.01/6.0%	↑ 3.09/4.0%	↑ 2.11/5.0%
II. MEDIUM-SIZED MODELS					
LLAMA3.1-8B-INSTRUCT					
LLAMA3.1-8B-INST (Grattafiori et al., 2024)	$6.46_{\pm 0.08}$	$0.00_{\pm 0.00}$	$19.27_{\pm 0.20}$	$49.06_{\pm 0.26}$	18.70
w/ RLPR (Yu et al., 2025)	$\underline{10.00}_{\pm 0.11}$	$\underline{0.96}_{\pm 0.03}$	$24.92_{\pm 0.21}$	$54.70_{\pm 0.22}$	22.64
w/ TTRL (Zuo et al., 2025)	$9.56_{\pm 0.03}$	$\underline{0.96}_{\pm 0.02}$	$\underline{32.08}_{\pm 0.12}$	$\mathbf{62.93}_{\pm 0.10}$	$\underline{26.38}$
w/ SCOPE (Ours)	$\mathbf{14.37}_{\pm 0.02}$	$\mathbf{1.44}_{\pm 0.04}$	$\mathbf{35.24}_{\pm 0.10}$	$\underline{61.67}_{\pm 0.13}$	**28.18**
Δ	↑ 4.81/50.3%	↑ 0.48/50.0%	↑ 3.16/9.9%	↓ 1.26/2.0%	↑ 1.80/6.8%
QWEN3-8B					
QWEN3-8B (Yang et al., 2025)	$26.45_{\pm 0.15}$	$20.67_{\pm 0.09}$	$59.50_{\pm 0.19}$	$83.66_{\pm 0.12}$	47.57
w/ EVOL-RL (Zhou et al., 2025)	$41.22_{\pm 0.17}$	$\underline{30.34}_{\pm 0.09}$	$69.62_{\pm 0.12}$	$\mathbf{91.70}_{\pm 0.04}$	$\underline{58.22}$
w/ CO-REWARDING-I (Zhang et al., 2025)	$28.39_{\pm 0.03}$	$21.74_{\pm 0.02}$	$\underline{71.39}_{\pm 0.03}$	$88.34_{\pm 0.01}$	52.47
w/ INTUITOR (Zhao et al., 2025)	$27.15_{\pm 0.13}$	$26.19_{\pm 0.10}$	$65.66_{\pm 0.15}$	$89.20_{\pm 0.06}$	52.05
w/ TTRL (Zuo et al., 2025)	$\underline{47.13}_{\pm 0.05}$	$27.40_{\pm 0.04}$	$68.55_{\pm 0.10}$	$89.74_{\pm 0.05}$	58.21
w/ SCOPE (Ours)	$\mathbf{52.70}_{\pm 0.02}$	$\mathbf{31.00}_{\pm 0.01}$	$\mathbf{74.09}_{\pm 0.03}$	$\underline{91.01}_{\pm 0.03}$	**62.20**
Δ	↑ 5.57/11.8%	↑ 3.60/13.1%	↑ 5.54/8.1%	↑ 1.27/1.4%	↑ 3.99/6.9%

Table 1: Comparison between the baselines and our method. In each column, the best results are **in bold**, and the second-best results are underlined. The Δ row reports the performance difference relative to the TTRL baseline.

across all evaluated settings. We detail the analysis based on model scales below.

Lightweight-sized Models. As shown in the first section of Table 1, despite the limited reasoning capacity of Qwen2.5-Math-1.5B and Qwen3-1.7B, SCOPE yields substantial performance gains over TTRL. For Qwen2.5-Math-1.5B, SCOPE achieves an average score of 41.36, surpassing TTRL (36.95) by an absolute margin of 4.41 (+11.9%). Notably, on the challenging AIME 2024 benchmark, SCOPE boosts the performance from 16.48 to 22.50, a remarkable relative improvement of 36.5%. Similarly, for Qwen3-1.7B, SCOPE reaches an improved average score of 44.02, outperforming TTRL across all four benchmarks. These results confirm that even for smaller models which typically struggle with self-verification, our subgroup-specific confidence weighting effectively filters out incorrect reasoning paths, enabling lightweight models to perform significantly beyond their parameter scale.

Medium-sized Models. The second section of Table 1 shows the results for medium-sized models, including LLaMA3.1-8B-Instruct and Qwen3-8B. On these stronger models, SCOPE also demonstrates remarkable performance. For LLaMA3.1-8B-Instruct, SCOPE achieves its largest relative gain on AIME 2024, improving performance from 9.56 of TTRL to 14.37, corresponding to a 50.3% improvement. Despite a minor regression on the easier MATH-500, SCOPE's substantial gains on competition-level datasets suggest it prioritizes complex reasoning over simpler tasks.On the strongest Qwen3-8B, SCOPE achieves absolute gains of 5.57 and 3.60 over TTRL on AIME 2024 and 2025, respectively. While maintaining comparable performance to EVOL-RL on the saturated MATH-500 benchmark, SCOPE establishes a dominant lead on competition-level tasks, surpassing EVOL-RL by 11.5% on AIME 2024. The overall averaged performance across all benchmarks reaches 62.20, exhibiting a 6.9% relative improvement over TTRL. These results suggest that stronger base models enable SCOPE to better leverage dense reward signals to rectify subtle errors in complex problem-solving scenarios.

4.3 Ablation Study

To demonstrate the effectiveness of our framework, we adopt several training settings: (1) ***w/o Conf***, which employs naive majority voting for pseudo-

Models	AIME 2024	AIME 2025
QWEN2.5-MATH-1.5B		
QWEN2.5-MATH-1.5B	7.92	3.12
w/ TTRL	16.48	9.86
w/ SCOPE	22.50	14.90
- *w/o Conf*	20.41 (-2.09)	11.77 (-3.13)
- *w/o Subgroup*	16.67 (-5.83)	11.05 (-3.85)
QWEN3-8B		
QWEN3-8B	26.45	20.67
w/ TTRL	47.13	27.40
w/ SCOPE	52.70	31.00
- *w/o Conf*	47.70 (-5.00)	28.36 (-2.64)
- *w/o Subgroup*	47.91 (-4.79)	26.92 (-4.08)

Table 2: Ablation study on step-wise confidence (*w/o Conf*) and automatic subgroup partition (*w/o Subgroup*).

label estimation; (2) ***w/o Subgroup***, which eliminates the subgroup partitioning strategy and computes the reward based on a single global consensus derived from the entire set of sampled outputs.

Table 2 shows the results. The consistent performance degradation upon removing either component validates the indispensability of our dual-granularity design. Specifically, the removal of subgroup partitioning leads to a sharp 5.83% decline for Qwen2.5-1.5B on AIME 2024, exposing the exploration bottleneck caused by monolithic supervision. Similarly, relying on naive majority voting yields a 5.00% deficit for Qwen3-8B on the same benchmark, confirming that naive majority voting is an unreliable proxy for reasoning quality. These findings indicate that model self-improvement hinges on the joint calibration of consensus scope and reward density.

5 Analyses

5.1 Impact of the Trade-off Parameter on Quality-Diversity Balance

To investigate the trade-off between reasoning quality and diversity, we analyze the trade-off parameter λ in Eq. 14 using Qwen3-8B. We vary λ from 0.0 to 1.0 and evaluate performance on AIME 2024 and AIME 2025. The results are shown in Figure 3.

When λ is set to 1.0, SCOPE relies solely on consensus quality. Although this setting already outperforms the TTRL baseline (horizontal dashed lines), performance saturates at 51.66% on AIME 2024. Introducing exploration by decreasing λ yields consistent gains, with peak performance at $\lambda = 0.5$, reaching 53.75% on AIME 2024 and 31.0% on AIME 2025. This indicates that while consensus is essential, encouraging exploration enables additional reasoning improvements beyond

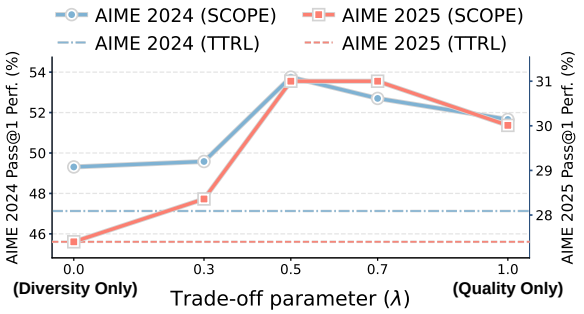

Figure 3: Analysis of the trade-off parameter λ.

pure consensus guidance.

Conversely, setting λ too low (e.g., $\lambda = 0$) results in a noticeable performance decline. Lacking the guidance of consensus quality, the optimization process is prone to over-exploration where the model drifts away from correct reasoning trajectories. This underscores the importance of jointly optimizing for both consensus alignment and exploration to achieve robust performance.

5.2 Impact of Confidence Granularity

Figure 4 compares our step-wise confidence strategy with average trace confidence, bottom-10% confidence, and tail-10% confidence (Fu et al., 2025) using Qwen2.5-Math-1.5B. Our method consistently outperforms all alternatives, achieving a 36.5% relative improvement on AIME 2024 and a larger 51.1% gain on the more challenging AIME 2025. In contrast, the bottom-10% strategy collapses (+0.0%), as sparse supervision overemphasizes the weakest step, penalizing difficult yet correct reasoning and discarding informative signals from the remainder of the chain.

Although the average trace strategy is more stable, it remains suboptimal due to error masking, where numerous trivial high-confidence steps obscure a critical intermediate mistake. Step-wise confidence overcomes this by enforcing dense, temporal supervision. By aligning reward resolution with step-level reasoning, our method ensures precise credit assignment, identifying and rectifying logical fallacies exactly where they occur without being smoothed out by global aggregation.

5.3 Efficacy of Automatic Subgroup Selection

We analyze the training dynamics of SCOPE and fixed subgroup partition strategies on Qwen2.5-Math-1.5B across AIME 2024 and AIME 2025 to investigate the effectiveness of automatic subgroup size selection. Figure 5 reveals a clear trade-off

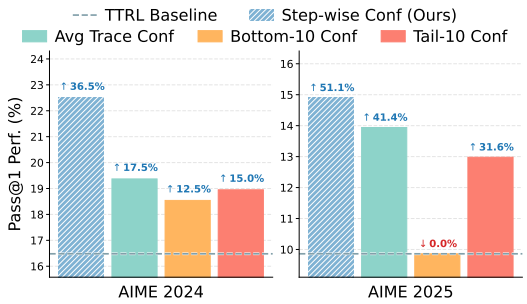

Figure 4: Impact analysis of confidence granularity. Comparison between SCOPE with our proposed step-wise confidence and alternative aggregation strategies.

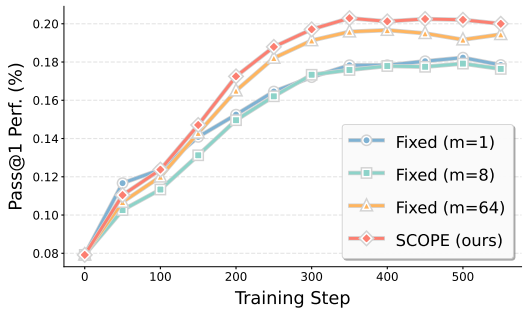

Figure 5: Impact analysis of subgroup size on training dynamics. Comparison between SCOPE with automatic subgroup size selection and variants with fixed subgroup sizes.

in consensus granularity. The atomized ($m = 1$) and small subgroup ($m = 8$) settings exhibit rapid initial growth but suffer from early saturation at a suboptimal level. This suggests that insufficient consensus amplifies noise and induces unreliable rewards and confirmation bias.

Conversely, while the global setting ($m = 64$) ensures stability, it converges more slowly due to an exploration bottleneck induced by static subgroup partition. In contrast, the automatic selection strategy consistently leads, achieving both faster convergence and higher peak performance. By dynamically balancing exploration and quality, it avoids the noise of small groups while mitigating the rigidity of global consensus, thereby maximizing sample efficiency.

5.4 Subgroup Partition Reduces Consensus Drift

To investigate whether subgroup partitioning reduces consensus drift compared with global consensus without subgrouping, we further analyze pseudo-label stability using Qwen2.5-Math-1.5B. We introduce *Pseudo-label Accuracy* (PLA), which measures the strict consistency between estimated consensus pseudo-labels and ground-truth labels during training. Higher PLA indicates lower pseudo-label noise and a more reliable consensus signal. We compare TTRL with fixed subgroup sizes and the automatic partition version of SCOPE, with results reported in Table 3.

The results show that SCOPE consistently improves PLA over TTRL across different subgroup settings, demonstrating that subgroup partitioning reduces consensus drift rather than amplifying pseudo-label noise. Notably, the automatic partition version achieves the highest PLA, outperforming TTRL by 20.81%. These results indicate

Method	PLA	Improvement
TTRL	25.42	–
SCOPE ($m = 1$)	26.75	5.24%
SCOPE ($m = 8$)	26.84	5.59%
SCOPE ($m = 64$)	29.57	16.33%
SCOPE (ours)	30.71	20.81%

Table 3: Analysis of pseudo-label accuracy under different subgroup sizes.

that subgroup partitioning improves pseudo-label stability and effectively mitigates consensus drift.

6 Related Work

RL for LLMs Reasoning. Reinforcement learning has emerged as a critical paradigm for enhancing the reasoning capabilities of LLMs (Zhang et al., 2023; DeepSeek-AI, 2025). Recent advancements focus on optimizing learning signals and training strategies. From the perspective of action space granularity, recent works have also explored extending single-token optimization to multi-token blocks to capture structural semantics (Xu et al., 2026). To improve sample efficiency, Wang et al. (2025d) introduced 1-shot RLVR, which selects high-quality examples based on historical variance to match the efficacy of large-scale training. For finer-grained credit assignment, Wang et al. (2025b) leveraged chain-of-thought entropy to identify critical tokens for targeted policy updates. In terms of data curation, Ye et al. (2025) proposed the Process Consistency Filter to harmonize noisy signals by filtering samples based on process–outcome consistency. Furthermore, employing adversarial strategies, Wu et al. (2025) introduced RLAC, where a critic generates verifiable rubrics to guide the generator's optimization. Despite these significant strides, most of these methods still rely on

substantial amounts of labeled data or ground-truth feedback during training.

Unsupervised RL. Unsupervised RL, which leverages self-derived signals without external annotation, has emerged as a promising direction for autonomous evolution (Sun et al., 2025; Ji et al., 2025; Chuang et al., 2025). Early explorations validated this paradigm through different methods (Wang et al., 2025a; Yuan et al., 2024). Following the success of DeepSeek-R1 (DeepSeek-AI, 2025), recent efforts have increasingly focused on circumventing the reliance on labeled data. For instance, Zuo et al. (2025) introduced TTRL, employing majority-voted labels as reward proxies—a mechanism further refined by EVOL-RL (Zhou et al., 2025) via novelty incentives and Co-rewarding (Zhang et al., 2025) through semantic consistency checks. Alternatively, other works exploit internal model states: Zhao et al. (2025) formulates self-certainty as an intrinsic reward for advantage estimation, while van Niekerk et al. (2025) utilize raw confidence scores as intrinsic feedback for preference optimization. However, relying solely on coarse-grained consensus or uncalibrated confidence signals often introduces noise and confirmation bias, failing to provide the fine-grained, reliable guidance necessary for solving complex reasoning tasks.

7 Conclusion

We propose SCOPE, a test-time reinforcement learning framework that mitigates confirmation bias and reward sparsity during unsupervised RL. By leveraging step-wise confidence and dynamic subgroup partitioning, SCOPE provides more reliable supervision and enables diverse, high-quality reasoning exploration. It achieves superior performance across representative reasoning benchmarks, consistently surpassing strong baselines.

Limitations

Despite significant performance gains, SCOPE has certain limitations. First, our step definition relies on heuristic segmentation based on newline characters. While this aligns with the standard output format of most reasoning models, it assumes a structured generation pattern. Second, the dynamic calculation of Pareto-optimal subgroups introduces roughly a 10% computational overhead. However, considering the substantial improvements in sample efficiency and final accuracy, we regard this as a highly favorable trade-off. Future work may extend this paradigm to longer-horizon and interactive agent settings, and explore more efficient test-time training dynamics to support robust self-evolution at scale.

Acknowledgments

This work was supported in parts by ICFCRT (W2441020), Guangdong Basic and Applied Basic Research Foundation (2026A1515011358), Shenzhen Natural Science Foundation (JCYJ2025 0604181610014), and Scientific Development Funds from Shenzhen University.

References

Eric Arazo, Diego Ortego, Paul Albert, Noel E O'Connor, and Kevin McGuinness. 2020. Pseudo-labeling and confirmation bias in deep semi-supervised learning. In *2020 International Joint Conference on Neural Networks (IJCNN)*. IEEE.

Mark Chen, Jerry Tworek, Heewoo Jun, Qiming Yuan, Henrique Ponde de Oliveira Pinto, Jared Kaplan, Harri Edwards, Yuri Burda, Nicholas Joseph, Greg Brockman, et al. 2021. Evaluating large language models trained on code. *arXiv preprint arXiv:2107.03374*.

Yung-Sung Chuang, Benjamin Cohen-Wang, Zejiang Shen, Zhaofeng Wu, Hu Xu, Xi Victoria Lin, James R. Glass, Shang-Wen Li, and Wen tau Yih. 2025. SelfCite: Self-supervised alignment for context attribution in large language models. In *Forty-second International Conference on Machine Learning*.

DeepSeek-AI. 2025. Deepseek-r1: Incentivizing reasoning capability in llms via reinforcement learning. *arXiv preprint arXiv:2501.12948*.

Yichao Fu, Xuewei Wang, Yuandong Tian, and Jiawei Zhao. 2025. Deep think with confidence. *arXiv preprint arXiv:2508.15260*.

Aaron Grattafiori, Abhimanyu Dubey, Abhinav Jauhri, Abhinav Pandey, Abhishek Kadian, Ahmad Al-Dahle, Aiesha Letman, Akhil Mathur, Alan Schelten, Alex Vaughan, et al. 2024. The llama 3 herd of models. *arXiv preprint arXiv:2407.21783*.

Dan Hendrycks, Collin Burns, Saurav Kadavath, Akul Arora, Steven Basart, Eric Tang, Dawn Song, and Jacob Steinhardt. 2021. Measuring mathematical problem solving with the math dataset. In *Proceedings of the Neural Information Processing Systems Track on Datasets and Benchmarks*, volume 1.

Weiyang Huang, Xuefeng Bai, Kehai Chen, Xinyang Chen, Yibin Chen, Weili Guan, and Min Zhang. 2026. Sat: Balancing reasoning accuracy and efficiency

with stepwise adaptive thinking. *arXiv preprint arXiv:2604.07922*.

Ke Ji, Junying Chen, Anningzhe Gao, Wenya Xie, Xiang Wan, and Benyou Wang. 2025. Unlocking LLMs' self-improvement capacity with autonomous learning for domain adaptation. In *Findings of the Association for Computational Linguistics: ACL 2025*, pages 21051–21067, Vienna, Austria. Association for Computational Linguistics.

Jia Li, Edward Beeching, Lewis Tunstall, Ben Lipkin, Roman Soletskyi, Shengyi Huang, Kashif Rasul, Longhui Yu, Albert Q Jiang, Ziju Shen, et al. 2024. Numinamath: The largest public dataset in ai4maths with 860k pairs of competition math problems and solutions. *Hugging Face repository*, 13(9):9.

Hunter Lightman, Vineet Kosaraju, Yuri Burda, Harrison Edwards, Bowen Baker, Teddy Lee, Jan Leike, John Schulman, Ilya Sutskever, and Karl Cobbe. 2024. Let's verify step by step. In *The Twelfth International Conference on Learning Representations*.

Chenwei Lou, Zewei Sun, Xinnian Liang, Meng Qu, Wei Shen, Wenqi Wang, Yuntao Li, Qingping Yang, and Shuangzhi Wu. 2025. AdaCoT: Pareto-optimal adaptive chain-of-thought triggering via reinforcement learning. *arXiv preprint arXiv:2505.11896*.

OpenAI. 2024. Openai o1 system card. *arXiv preprint arXiv:2412.16720*.

Vilfredo Pareto. 1964. *Cours d'économie politique*, volume 1. Librairie Droz.

Viraj Prabhu, Shivam Khare, Deeksha Kartik, and Judy Hoffman. 2021. Sentry: Selective entropy optimization via committee consistency for unsupervised domain adaptation. In *Proceedings of the IEEE/CVF International Conference on Computer Vision (ICCV)*, pages 8558–8567.

Zhihong Shao, Peiyi Wang, Qihao Zhu, Runxin Xu, Junxiao Song, Xiao Bi, Haowei Zhang, Mingchuan Zhang, YK Li, Yang Wu, et al. 2024. Deepseekmath: Pushing the limits of mathematical reasoning in open language models. *arXiv preprint arXiv:2402.03300*.

Guangming Sheng, Chi Zhang, Zilingfeng Ye, Xibin Wu, Wang Zhang, Ru Zhang, Yanghua Peng, Haibin Lin, and Chuan Wu. 2025. Hybridflow: A flexible and efficient rlhf framework. In *EuroSys*, pages 1279–1297.

Yi Su, Dian Yu, Linfeng Song, Juntao Li, Haitao Mi, Zhaopeng Tu, Min Zhang, and Dong Yu. 2025. Crossing the reward bridge: Expanding rl with verifiable rewards across diverse domains. *arXiv preprint arXiv:2503.23829*.

Yutao Sun, Mingshuai Chen, Tiancheng Zhao, Ruochen Xu, Zilun Zhang, and Jianwei Yin. 2025. The self-improvement paradox: Can language models bootstrap reasoning capabilities without external scaffolding? In *Findings of the Association for Computational Linguistics: ACL 2025*, pages 6501–6512, Vienna, Austria. Association for Computational Linguistics.

Xinyu Tang, Zhenduo Zhang, Yurou Liu, Wayne Xin Zhao, Zujie Wen, Zhiqiang Zhang, and Jun Zhou. 2025. Towards high data efficiency in reinforcement learning with verifiable reward. *arXiv preprint arXiv:2509.01321*.

Carel van Niekerk, Renato Vukovic, Benjamin Matthias Ruppik, Hsien-chin Lin, and Milica Gašić. 2025. Post-training large language models via reinforcement learning from self-feedback. *arXiv preprint arXiv:2507.21931*.

Pinzheng Wang, Juntao Li, Zecheng Tang, Haijia Gui, and Min zhang. 2025a. Improving rationality in the reasoning process of language models through self-playing game. In *Forty-second International Conference on Machine Learning*.

Shenzhi Wang, Le Yu, Chang Gao, Chujie Zheng, Shixuan Liu, Rui Lu, Kai Dang, Xiong-Hui Chen, Jianxin Yang, Zhenru Zhang, Yuqiong Liu, An Yang, Andrew Zhao, Yang Yue, Shiji Song, Bowen Yu, Gao Huang, and Junyang Lin. 2025b. Beyond the 80/20 rule: High-entropy minority tokens drive effective reinforcement learning for LLM reasoning. In *The Thirty-ninth Annual Conference on Neural Information Processing Systems*.

Weiqin Wang, Yile Wang, and Hui Huang. 2025c. Ranked voting based self-consistency of large language models. In *Findings of the Association for Computational Linguistics: ACL 2025*, pages 14410–14426, Vienna, Austria. Association for Computational Linguistics.

Yiping Wang, Qing Yang, Zhiyuan Zeng, Liliang Ren, Liyuan Liu, Baolin Peng, Hao Cheng, Xuehai He, Kuan Wang, Jianfeng Gao, Weizhu Chen, Shuohang Wang, Simon Shaolei Du, and yelong shen. 2025d. Reinforcement learning for reasoning in large language models with one training example. In *The Thirty-ninth Annual Conference on Neural Information Processing Systems*.

Xumeng Wen, Zihan Liu, Shun Zheng, Zhijian Xu, Shengyu Ye, Zhirong Wu, Xiao Liang, Yang Wang, Junjie Li, Ziming Miao, et al. 2025. Reinforcement learning with verifiable rewards implicitly incentivizes correct reasoning in base llms. *arXiv preprint arXiv:2506.14245*.

Mian Wu, Gavin Zhang, Sewon Min, Sergey Levine, and Aviral Kumar. 2025. RLAC: Reinforcement learning with adversarial critic for free-form generation tasks. *arXiv preprint arXiv:2511.01758*.

Mufan Xu, Kehai Chen, Xuefeng Bai, Zhengyu Niu, Muyun Yang, Tiejun Zhao, and Min Zhang. 2026. Beyond token-level policy gradients for complex reasoning with large language models. *arXiv preprint arXiv:2602.14386*.

An Yang, Anfeng Li, Baosong Yang, Beichen Zhang, Binyuan Hui, Bo Zheng, Bowen Yu, Chang Gao, Chengen Huang, Chenxu Lv, et al. 2025. Qwen3 technical report. *arXiv preprint arXiv:2505.09388*.

An Yang, Beichen Zhang, Binyuan Hui, Bofei Gao, Bowen Yu, Chengpeng Li, Dayiheng Liu, Jianhong Tu, Jingren Zhou, Junyang Lin, et al. 2024. Qwen2.5-math technical report: Toward mathematical expert model via self-improvement. *arXiv preprint arXiv:2409.12122*.

Chenlu Ye, Zhou Yu, Ziji Zhang, Hao Chen, Narayanan Sadagopan, Jing Huang, Tong Zhang, and Anurag Beniwal. 2025. Beyond correctness: Harmonizing process and outcome rewards through rl training. *arXiv preprint arXiv:2509.03403*.

Tianyu Yu, Bo Ji, Shouli Wang, Shu Yao, Zefan Wang, Ganqu Cui, Lifan Yuan, Ning Ding, Yuan Yao, Zhiyuan Liu, et al. 2025. RLPR: Extrapolating rlvr to general domains without verifiers. *arXiv preprint arXiv:2506.18254*.

Weizhe Yuan, Richard Yuanzhe Pang, Kyunghyun Cho, Xian Li, Sainbayar Sukhbaatar, Jing Xu, and Jason E Weston. 2024. Self-rewarding language models. In *Forty-first International Conference on Machine Learning*.

Weihao Zeng, Yuzhen Huang, Qian Liu, Wei Liu, Keqing He, Zejun MA, and Junxian He. 2025. SimpleRL-zoo: Investigating and taming zero reinforcement learning for open base models in the wild. In *Second Conference on Language Modeling*.

Yifan Zhang, Jingqin Yang, Yang Yuan, and Andrew Chi-Chih Yao. 2023. Cumulative reasoning with large language models. *Transactions on Machine Learning Research; arXiv preprint arXiv:2308.04371*.

Zizhuo Zhang, Jianing Zhu, Xinmu Ge, Zihua Zhao, Zhanke Zhou, Xuan Li, Xiao Feng, Jiangchao Yao, and Bo Han. 2025. Co-rewarding: Stable self-supervised rl for eliciting reasoning in large language models. *arXiv preprint arXiv:2508.00410*.

Xuandong Zhao, Zhewei Kang, Aosong Feng, Sergey Levine, and Dawn Song. 2025. Learning to reason without external rewards. *arXiv preprint arXiv:2505.19590*.

Yifan Zhong, Chengdong Ma, Xiaoyuan Zhang, Ziran Yang, Haojun Chen, Qingfu Zhang, Siyuan Qi, and Yaodong Yang. 2024. Panacea: Pareto alignment via preference adaptation for llms. In *Advances in Neural Information Processing Systems*, volume 37, pages 75522–75558. Curran Associates, Inc.

Yujun Zhou, Zhenwen Liang, Haolin Liu, Wenhao Yu, Kishan Panaganti, Linfeng Song, Dian Yu, Xiangliang Zhang, Haitao Mi, and Dong Yu. 2025. Evolving language models without labels: Majority drives selection, novelty promotes variation. *arXiv preprint arXiv:2509.15194*.

Yuxin Zuo, Kaiyan Zhang, Li Sheng, Shang Qu, Ganqu Cui, Xuekai Zhu, Haozhan Li, Yuchen Zhang, Xinwei Long, Ermo Hua, Biqing Qi, Youbang Sun, Zhiyuan Ma, Lifan Yuan, Ning Ding, and Bowen Zhou. 2025. TTRL: Test-time reinforcement learning. In *The Thirty-ninth Annual Conference on Neural Information Processing Systems*.

A Checkpoints of Models

The checkpoints of open-source models in our experiments are shown in Table 4.

Model	Resource Link
QWEN SERIES	
QWEN2.5-MATH-1.5B	Qwen/Qwen2.5-Math-1.5B
QWEN3-1.7B	Qwen/Qwen3-1.7B
QWEN3-8B	Qwen/Qwen3-8B
LLAMA SERIES	
LLAMA3.1-8B-INSTRUCT	meta-llama/Llama-3.1-8B-Instruct

Table 4: Checkpoints of open-source models in our experiments.

B Example of Datasets

Table 5 provides representative examples from the evaluation datasets along with their respective sizes.

Type	Content
AIME 2024 (30)	
Question	Every morning Aya goes for a 9-kilometer-long walk and stops at a coffee shop afterwards. When she walks at a constant speed of s kilometers per hour, the walk takes her 4 hours, including t minutes spent in the coffee shop. When she walks $s+2$ kilometers per hour, the walk takes her 2 hours and 24 minutes, including t minutes spent in the coffee shop. Suppose Aya walks at $s+\frac{1}{2}$ kilometers per hour. Find the number of minutes the walk takes her, including the t minutes spent in the coffee shop.
Answer	$\boxed{204}$
AIME 2025 (30)	
Question	Find the sum of all integer bases $b > 9$ for which 17_b is a divisor of 97_b.
Answer	$\boxed{70}$
AMC (83)	
Question	$\frac{m}{n}$ is the Irreducible fraction value of $$3+\frac{1}{3+\frac{1}{3+\frac{1}{3}}}$$, what is the value of $m+n$?
Answer	$\boxed{142.0}$
MATH-500 (500)	
Question	Convert the point $(0,3)$ in rectangular coordinates to polar coordinates. Enter your answer in the form (r,θ), where $r>0$ and $0 \le \theta < 2\pi$.
Answer	$\boxed{\left(3, \frac{\pi}{2}\right)}$

Table 5: Examples of questions and answers from the evaluation datasets.

System Prompt

Please reason step by step, and put your final answer within \boxed{}.

C Implementation Details

Training Configuration We implement our method using the *Volcano Engine Reinforcement Learning for LLMs* framework (Sheng et al., 2025). Regarding hyperparameters, we employ the AdamW optimizer for the policy model, utilizing a cosine learning rate schedule with a peak value of 5×10^{-7}. During the rollout phase, we sample 64 responses per prompt using a temperature of 0.6 (adjusted to 1.0 for Qwen2.5-Math). For label estimation, we perform bootstrap sampling with 32 samples for each subgroup and subsequently utilize all 64 responses for training. The maximum generation length is set to 3,072 tokens.

Prompt for Training For all experiments, we employed a standardized system prompt to regulate the output format, explicitly requiring the model to articulate a step-by-step reasoning process followed by a clearly delimited final answer (Zeng et al., 2025):

Evaluation Configuration We apply our method to each benchmark individually, setting the maximum generation length to 3072 tokens unless otherwise specified. For the main experiments, following the protocol of DeepSeek-R1 (DeepSeek-AI, 2025), we adopt the pass@k metric (Chen et al., 2021) and report pass@1 using non-zero temperature sampling. Specifically, we generate 16 responses (4 for models with 32k context) per question using a temperature of 0.6 and a top-p value of 0.95. The pass@1 score is computed as:

$$\text{pass@1} = \frac{1}{k}\sum_{i=1}^{k} p_i, \tag{16}$$

where p_i indicates correctness of the i-th response. where p_i indicates whether the i-th response is correct.

D Case Study

We present the generation outputs for the same question shown in Figure 6 from four different models: (1) the backbone model (Figure 7); (2) the model after TTRL training (Figure 8); (3) the model after full SCOPE training (Figure 9).

Question

Every morning Aya goes for a 9-kilometer-long walk and stops at a coffee shop afterwards. When she walks at a constant speed of s kilometers per hour, the walk takes her 4 hours, including t minutes spent in the coffee shop. When she walks $s+2$ kilometers per hour, the walk takes her 2 hours and 24 minutes, including t minutes spent in the coffee shop. Suppose Aya walks at $s+\frac{1}{2}$ kilometers per hour. Find the number of minutes the walk takes her, including the t minutes spent in the coffee shop.

Figure 6: A question from AIME 2024.

These correspond to solution1, solution2, and solution3, respectively. The backbone model (solution1) fails due to a critical logic error: adding total time instead of the break duration and hallucinates a final answer of `120`. The model trained with TTRL (solution2), although producing the correct numerical answer, exhibits clear flaws in mathematical modeling. Specifically: (1) in the **equation-formulation stage**, it erroneously subtracts the coffee-break time from the walking time (e.g., $\frac{9\times 60}{s} - t = 240$); (2) in the **intermediate-calculation stage**, this mistake leads to an impossible negative duration ($t = -24$ minutes); and (3) in the **Python-execution stage**, the error is obscured by applying `abs()`, which masks the incorrect reasoning rather than correcting it. These incorrect components are highlighted with red boxes in the annotated solution. In contrast, SCOPE (Solution 3) demonstrates superior reasoning by identifying the invariance of break time. It eliminates variables to form a concise quadratic equation, grasping the true physical relationships without erroneous patching. It efficiently eliminates the variable t to form a concise quadratic equation, showcasing that SCOPE enables the model to grasp the true physical relationships within the problem.

E Use of AI Assistants

AI assistants were used solely for translation and linguistic polishing purposes. They did not contribute to the generation of research conclusions, experimental results, or the core technical content of this work.

Solution1

Let's solve the problem step by step using Python and SymPy.

1. Understand the Problem:

- When Aya walks at a speed of s km/h, the total time taken for the walk and the coffee shop break is 4 hours.
- When Aya walks at a speed of $s+2$ km/h, the total time taken for the walk and the coffee shop break is 2 hours and 24 minutes (which is 2.4 hours).
- We need to find the time taken when Aya walks at a speed of $s+\frac{1}{2}$ km/h.

2. Formulate the Equations:

- Let t be the time spent in the coffee shop break in minutes.
- When Aya walks at s km/h, the time taken for the walk is $\frac{9}{s}$ hours, which is $\frac{9}{s} \times 60$ minutes. So the total time is $\frac{9}{s} \times 60 + t = 4 \times 60 = 240$ minutes.
- When Aya walks at $s+2$ km/h, the time taken for the walk is $\frac{9}{s+2}$ hours, which is $\frac{9}{s+2} \times 60$ minutes. So the total time is $\frac{9}{s+2} \times 60 + t = 2.4 \times 60 = 144$ minutes.

3. Set Up the Equations:

- From the first condition: $\frac{9}{s} \times 60 + t = 240$
- From the second condition: $\frac{9}{s+2} \times 60 + t = 144$

4. Solve the Equations:

- Subtract the second equation from the first to eliminate t:

$$\frac{9}{s} \times 60 + t - \left(\frac{9}{s+2} \times 60 + t\right) = 240 - 144$$

- Simplify and solve for s:

$$\frac{9}{s} \times 60 - \frac{9}{s+2} \times 60 = 96$$

$$9 \times 60 \left(\frac{1}{s} - \frac{1}{s+2}\right) = 96$$

$$540 \left(\frac{s+2-s}{s(s+2)}\right) = 96 \implies \frac{1080}{s(s+2)} = 96$$

$$1080 = 96s^2 + 192s$$

$$96s^2 + 192s - 1080 = 0$$

- Divide the whole equation by 24:

$$4s^2 + 8s - 45 = 0$$

- Solve this quadratic equation using the quadratic formula $s = \frac{-b \pm \sqrt{b^2-4ac}}{2a}$, where $a = 4$, $b = 8$, and $c = -45$.

5. Find the Speed and Time:

- Solve the quadratic equation to find s.
- Use the value of s to find the time taken when walking at $s+\frac{1}{2}$ km/h.

Let's implement this in Python:

```python
import sympy as sp
# Define the variable
s = sp.symbols('s')
# Define the quadratic equation
equation = 4*s**2 + 8*s - 45
# Solve the quadratic equation
solutions = sp.solve(equation, s)
# We need the positive solution
s_value = [sol for sol in solutions if sol > 0][0]
# Calculate the time taken when walking at s + 1/2 km/h
time_walk = (9 / (s_value + 0.5)) * 60
# The total time including the coffee shop break
total_time = time_walk + 144
# Convert the total time from minutes to hours and then to minutes
total_time_minutes = total_time
print(total_time_minutes)
```

Output: `120`

The number of minutes the walk takes Aya, including the coffee shop break, when she walks at $s+\frac{1}{2}$ kilometers per hour is $\boxed{120}$.

Figure 7: Solution from Qwen2.5-Math-1.5B.

Solution2

Let's break down the problem step-by-step and solve it using Python and SymPy.

1. Understand the Problem:

- When Aya walks at a speed of s km/h, the walk takes her 4 hours, including t minutes spent in the coffee shop.
- When she walks at a speed of $s+2$ km/h, the walk takes her 2 hours and 24 minutes, including t minutes spent in the coffee shop.
- We need to find the number of minutes the walk takes her, including the t minutes spent in the coffee shop, when she walks at $s+\frac{1}{2}$ km/h.

2. Formulate the Equations:

- The total time spent walking is 4 hours when the speed is s km/h.
- The total time spent walking is $2+\frac{24}{60}=2.4$ hours when the speed is $s+2$ km/h.
- The distance Aya walks is 9 km in both cases.
- Let t be the time spent in the coffee shop in minutes. Then the walking time is $4\times 60-t$ minutes when the speed is s km/h, and $2.4\times 60-t$ minutes when the speed is $s+2$ km/h.

3. Set Up the Equations:

- When the speed is s km/h, the walking time is $\frac{9}{s}\times 60-t=240-t$ minutes.
- When the speed is $s+2$ km/h, the walking time is $\frac{9}{s+2}\times 60-t=144-t$ minutes.
- So we have the following equations:

$$\frac{9\times 60}{s}\boxed{\text{- t}}=240$$

$$\frac{9\times 60}{s+2}\boxed{\text{- t}}=144$$

4. Solve the Equations:

- From the first equation, we get: $t=\frac{540}{s}-240$.
- From the second equation, we get: $t=\frac{540}{s+2}-144$.
- Equate the two expressions for t and simplify:

$$\frac{540}{s}-240=\frac{540}{s+2}-144$$

$$540\left(\frac{s+2-s}{s(s+2)}\right)=96 \implies 1080=96s(s+2)$$

$$4s^2+8s-45=0$$

- Solve the quadratic equation using the quadratic formula:

$$s=\frac{-8\pm\sqrt{64+720}}{8}=\frac{20}{8}=2.5 \text{ (since } s>0)$$

5. Find the Time Spent in the Coffee Shop:

- Substitute $s=2.5$ into the equation for t:

$$t=\frac{540}{2.5}-240=216-240=\boxed{\text{-24}}$$

- $t=24$ minutes (taking magnitude).

6. Find the Time for the Walk at $s+\frac{1}{2}$ km/h:

- The walking time is $\frac{9}{2.5+0.5}\times 60=180$ minutes.
- Including the t minutes spent in the coffee shop, total time is $180+24=204$ minutes.

Let's implement this in Python to verify our solution.

```
import sympy as sp
s = sp.symbols('s')
# Define equations based on derivation
eq1 = sp.Eq(540/s - 240, 540/(s + 2) - 144)     <- ERROR: flawed time equation
solution = sp.solve(eq1, s)
s_val = [sol.evalf() for sol in solution if sol > 0][0]
t = abs((540 / s_val) - 240)                     <- ERROR: masking negative time with abs()
total = (9 / (s_val + 0.5)) * 60 + t
print(total)
```

Output: `204.000000000000`

The total time Aya spends walking, including the time spent in the coffee shop, when she walks at a speed of $s+\frac{1}{2}$ km/h is $\boxed{204}$ minutes.

Figure 8: Solution after training process of TTRL.

Solution3

To solve this problem, we need to determine the time Aya spends walking and the time she spends in the coffee shop. Let's break it down step-by-step.

1. Determine the time spent in the coffee shop:

- When Aya walks at a speed of s km/h, the total time for the walk including the coffee shop break is 4 hours. Since the walk itself takes $\frac{9}{s}$ hours, the time spent in the coffee shop is $4 - \frac{9}{s}$ hours.
- When Aya walks at a speed of $s + 2$ km/h, the total time for the walk including the coffee shop break is 2 hours and 24 minutes, which is 2.4 hours. The time spent in the coffee shop is $2.4 - \frac{9}{s+2}$ hours.

Since the time spent in the coffee shop is the same in both cases, we can set up the following equation:

$$4 - \frac{9}{s} = 2.4 - \frac{9}{s+2}$$

2. Solve for s: Let's solve this equation step-by-step.

$$\begin{aligned}
4 - \frac{9}{s} &= 2.4 - \frac{9}{s+2} \\
4 - 2.4 &= \frac{9}{s} - \frac{9}{s+2} \\
1.6 &= 9\left(\frac{1}{s} - \frac{1}{s+2}\right) \\
1.6 &= 9\left(\frac{(s+2) - s}{s(s+2)}\right) \\
1.6 &= 9\left(\frac{2}{s(s+2)}\right) \\
1.6 &= \frac{18}{s(s+2)} \\
1.6s(s+2) &= 18 \\
1.6s^2 + 3.2s - 18 &= 0 \\
16s^2 + 32s - 180 &= 0 \\
4s^2 + 8s - 45 &= 0
\end{aligned}$$

We can solve this quadratic equation using the quadratic formula $s = \frac{-b \pm \sqrt{b^2 - 4ac}}{2a}$, where $a = 4$, $b = 8$, and $c = -45$.

$$\begin{aligned}
s &= \frac{-8 \pm \sqrt{8^2 - 4 \cdot 4 \cdot (-45)}}{2 \cdot 4} \\
s &= \frac{-8 \pm \sqrt{64 + 720}}{8} \\
s &= \frac{-8 \pm \sqrt{784}}{8} = \frac{-8 \pm 28}{8} \\
s &= \frac{20}{8} = 2.5 \quad \text{or} \quad s = \frac{-36}{8} = -4.5
\end{aligned}$$

Since s represents a speed, it must be positive. Therefore, $s = 2.5$ km/h.

3. Determine the time spent in the coffee shop:

- When Aya walks at $s = 2.5$ km/h, the time spent in the coffee shop is $4 - \frac{9}{2.5} = 4 - 3.6 = 0.4$ hours, which is $0.4 \times 60 = 24$ minutes.

4. Determine the time for the walk at $s + \frac{1}{2} = 3$ km/h:

- The time for the walk is $\frac{9}{3} = 3$ hours.
- Including the 24 minutes spent in the coffee shop, the total time is $3 + 0.4 = 3.4$ hours, which is $3.4 \times 60 = 204$ minutes.

The final answer is $\boxed{204}$.

Figure 9: Solution after training process of SCOPE.